Journal of the Physical Society of Japan
Vol. 51, No. 12, December, 1982, pp. 3893–3899

Self-Consistent Results for a GaAs/$Al_xGa_{1-x}As$ Heterojunction. I. Subband Structure and Light-Scattering Spectra

Tsuneya ANDO

Institute of Applied Physics, University of Tsukuba, Sakura, Ibaraki 305

(Received July 7, 1982)

The subband structure of a two-dimensional electron system at a GaAs/$Al_xGa_{1-x}As$ heterojunction interface is calculated. Many-body exchange and correlation effects are taken into account in the local density-functional approximation. They are shown to be unimportant but not negligibly small. Spectra of light scatterings are also calculated. Results are in reasonable agreement with existing experiments.

§1. Introduction

There has been much interest in electronic properties of two-dimensional systems. Space-charge layers, mainly on Si surfaces, have been the typical physical realization of a two-dimensional electron gas and most extensively been studied.[1] Recently, the evolution of molecular-beam epitaxy combined with the use of the modulation doping technique made it possible to achieve a new two-dimensional system at the semiconductor heterojunction interface between GaAs and $Al_xGa_{1-x}As$.[1] In this system the wide gap material ($Al_xGa_{1-x}As$) is selectively n doped, while the narrow gap material (GaAs) is essentially free of impurities. Under equilibrium conditions, electrons in donor levels of $Al_xGa_{1-x}As$ are transferred to the GaAs layer, leading to considerable band bending and forming a two-dimensional electron gas in GaAs. The spatial separation between electrons and charged donors is considered to be responsible for extremely high low-temperature mobility in this system. The purpose of the present series of papers is to present results of theoretical study of electronic properties of such a two-dimensional system at GaAs/$Al_xGa_{1-x}As$ heterojunction. This first paper is concerned with the problem related to the subband structure.

There have been many theoretical and experimental investigations on the subband structure in inversion and accumulation layers on Si surfaces.[1] It is now well-established that a self-consistent calculation based on the effective-mass approximation explains observed subband energy separations and spectra of intersubband optical transitions if many-body exchange and correlation effects are properly taken into account. Calculations have been extended to space-charge layers on surfaces of III-V compound semiconductors and other materials.[1] A self-consistent calculation has been performed also in GaAs/$Al_xGa_{1-x}As$ superlattices.[2,3] In this paper we apply the same method used for the superlattices to the single heterojunction and calculate the subband structure and light scattering spectra.

In §2 the method of calculation is briefly described and results are presented. Effects of the nonparabolicity of the GaAs conduction band are also discussed. The results are compared with existing experiments. Spectra of resonant light scatterings are calculated and will be shown to explain experiments in §3. A brief summary and a conclusion are given in §4.

§2. Subband Structure

2.1 Method of calculation

As far as the subband structure is concerned, the heterojunction is almost equivalent to the usual inversion layer on semiconductor surfaces. Only difference is that the wave function has a nonvanishing amplitude in the $Al_xGa_{1-x}As$ layer because the barrier height V_0 is not infinitely large ($V_0 \sim x$ in units of eV). Therefore, we cannot use the usual boundary condition that the envelope function vanishes at the interface, which will be chosen at

$z=0$. In previous work for superlattices the envelope functions of GaAs ($z>0$) and Al_x-$Ga_{1-x}As$ ($z<0$) have been smoothly matched at $z=0$. In this paper we employ a more refined treatment proposed recently.[4] In this theory the boundary condition for the envelope functions $\zeta_A(z)$ and $\zeta_B(z)$ of two materials A and B occupying left and right half-spaces, respectively, is written as

$$\begin{bmatrix} \zeta_B(0) \\ \nabla\zeta_B(0) \end{bmatrix} = \begin{bmatrix} t_{11} & t_{12} \\ t_{21} & t_{22} \end{bmatrix} \begin{bmatrix} \zeta_A(0) \\ \nabla\zeta_A(0) \end{bmatrix}, \quad (2.1)$$

where $\nabla\zeta = a\partial\zeta/\partial z$ with a being the lattice constant. The matrix $T_{BA}=(t_{ij})$ may be called an "interface matrix". The conservation of flux requires $|T_{BA}|=m_B/m_A$ where m_A and m_B are the effective masses. For GaAs (A) and $Al_xGa_{1-x}As$ (B) interfaces, T_{BA} has been calculated within a simplified LCAO approximation as $t_{12}=t_{21}=0$, $t_{11}=(E_g m'/E_g' m)^{1/2}$, and $t_{22}=(E_g' m'/E_g m)^{1/2}$, where m and E_g are the effective mass and the band gap, respectively, of GaAs and m' and E_g' are the corresponding quantities in $Al_xGa_{1-x}As$.[4]

The envelope function satisfies

$$\left[-\frac{\hbar^2}{2m_z}\frac{d^2}{dz^2}+\frac{\hbar^2}{2m_z}\boldsymbol{k}^2+V(z)\right]\zeta_{i\boldsymbol{k}}(z)=E_i(\boldsymbol{k})\zeta_{i\boldsymbol{k}}(z), \quad (2.2)$$

where $m_z=m$ for $z>0$ and $m_z=m'$ for $z<0$. The potential $V(z)$ is written as

$$V(z)=V_0\theta(-z)+v_H(z)+v_{xc}(z), \quad (2.3)$$

where $\theta(x)$ is the step function and the Hartree potential $v_H(z)$ is

$$v_H(z)=\frac{4\pi e^2}{\kappa}\int^z dz\int^{z'} dz''\, n(z'')+\frac{4\pi e^2}{\kappa}N_{depl}z, \quad (2.4)$$

where κ is the static dielectric constant, $n(z)$ is the electron density distribution, and N_{depl} is the concentration of fixed space charges in the GaAs depletion layer. The last term of eq. (2.3) is the local exchange-correlation potential which describes many-body corrections. We use here an expression parameterized by Gunnarson and Lundqvist[5] for the effective mass m_z and the static dielectric constant κ. This means that we neglect dynamical nature of electron-phonon interaction which might be important in this system. Kawamoto *et al.*[6,7] studied effects of electron-phonon interactions in inversion layers on polar materials. According to their results,[6] the present approximation slightly underestimates many-body corrections to the subband energy separations. However, this does not cause a serious problem because the many-body effect itself is not so important in the present GaAs/$Al_xGa_{1-x}As$ system. Equation (2.2) shows that the mass difference of m and m' causes the wave function $\zeta(z)$ to be dependent on the wave vector $\boldsymbol{k}$ parallel to the interface and the two-dimensional dispersion relation to deviate from $\hbar^2k^2/2m$. However, this effect turns out to be quite small and will completely be neglected for the calculation. That is, $\hbar^2k^2/2m_z$ in eq. (2.2) is replaced by $\hbar^2k^2/2m$. We shall return to this point later in connection with the enhancement of the effective mass.

2.2 *Results and comparison with experiments*

Figure 1 gives an example of calculated density distribution $n(z)$, potential energy $V(z)$, and bottom energies of low-lying subbands E_i for the Al content $x=0.3$. The electron concentration N_s is 5×10^{11} cm^{-2} and $N_{depl}=5\times10^{10}$ cm^{-2} corresponding to a p-type GaAs having an impurity concentration $N_A-N_D\sim10^{14}$ cm^{-3}. The other parameters are $\kappa=12.9$, $E_g=1.52$ eV, $E_g'=1.89$ eV, and $V_0=300$ meV. It is seen that the exchange and correlation are not so important in the present system as in Si inversion and accumulation layers.[1] The effect of discontinuity of the envelope function is also unimportant. The figure shows

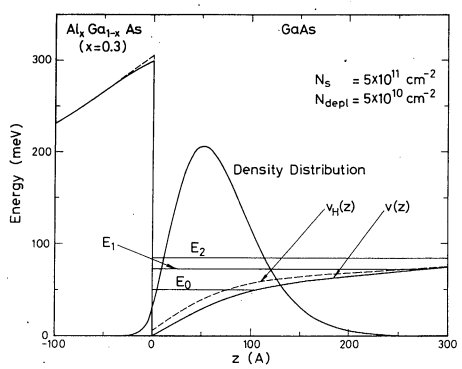

Fig. 1. An example of the calculated density distribution of electrons, self-consistent potential, bottoms of the low-lying subbands for $N_s=5\times10^{11}$ cm^{-2} and $N_{depl}=5\times10^{10}$ cm^{-2}. The Al content x of $Al_xGa_{1-x}As$ is 0.3. The dashed line represents the Hartree part of the potential $v_H(z)$. The difference between $v(z)$ and $v_H(z)$ represents the local exchange-correlation potential.

further that the average position of electrons is shifted to the negative z direction by about 20 A from the value obtained by assuming an infinitely high barrier height in the $Al_xGa_{1-x}As$ layer. This shift seems rather insensitive to N_s as long as only the lowest subband (E_0) is occupied by electrons.

Calculated subband energy separations $E_{i0}=E_i-E_0$ are plotted against N_s in Fig. 2 for the same values of the parameters as in Fig. 1. The corresponding results calculated in the Hartree approximation are also shown. Many-body exchange and correlation effects are not crucial although they are not negligibly small. The first excited subband starts to be occupied by electrons at $N_s=7.3\times10^{11}$ cm^{-2}, where a discontinuity appears in the variation of E_{i0} with N_s owing to the increase of the density of states after the excited subband is occupied. The energy separations especially between excited subbands depend strongly on N_{depl}. Figure 3 shows similar results for smaller N_{depl}, i.e. $N_{depl}=1\times10^9$ cm^{-2}. Such a small N_{depl} corresponds to the accumulation case (n-type GaAs) or quasi-accumulation cases

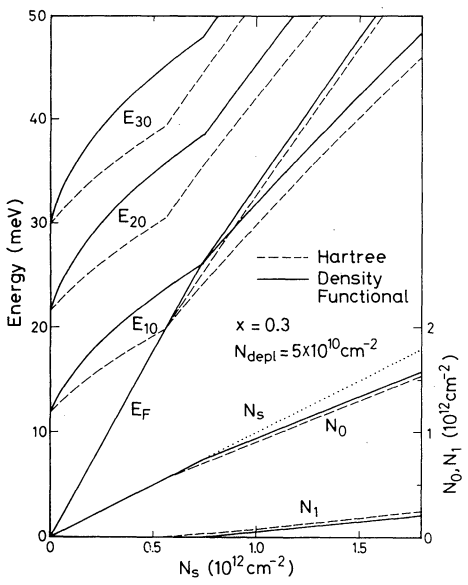

Fig. 2. Calculated subband energies measured from the bottom of the lowest subband E_0 for $N_{depl}=5\times10^{10}$ cm^{-2} and $x=0.3$. The solid and dashed lines represent the results calculated in the density-functional and Hartree approximation, respectively. The Fermi energy measured from the bottom of the lowest subband and the electron concentrations of the subbands are also plotted.

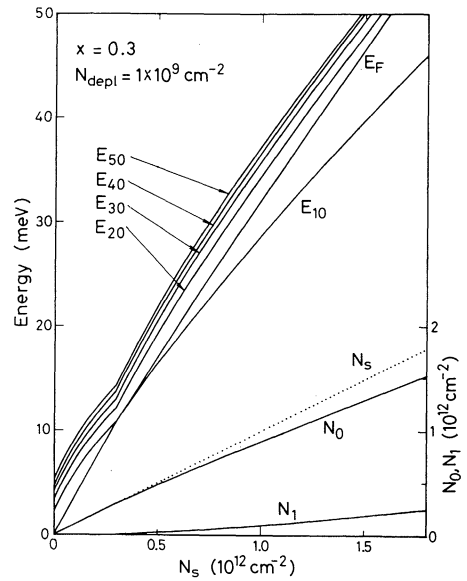

Fig. 3. Calculated subband energies measured from the bottom of the lowest subband E_0 for a quasi-accumulation case ($N_{depl}=1\times10^9$ cm^{-2}) and $x=0.3$. Only the results calculated in the density-functional approximation are shown. The second subband becomes occupied by electrons already at $N_s=3\times10^{11}$ cm^{-2}.

under exposure of band gap radiations. The Fermi level reaches the second subband already at $N_s=3\times10^{11}$ cm^{-2}. Similar calculations for different x (between 0.2 and 0.4) reveal that the energy levels, especially mutual energy separations, are rather insensitive to the barrier height V_0.

Störmer *et al.*[8] measured Shubnikov-de Haas oscillations at low temperatures and determined the electron concentration of the first excited subband as $N_1=2\times10^{11}$ cm^{-2} at $N_s=1.6\times10^{12}$ cm^{-2} for the quasi-accumulation case. The present calculation gives $N_1=2.1\times10^{11}$ cm^{-2} in good agreement with the experiment. Further, more recent experiments[9] give N_1 which lies very close to that shown in Fig. 3 for N_s between 1.2×10^{12} and 1.5×10^{12} cm^{-2}.

Cyclotron resonance have been observed in this system.[8-11] Störmer *et al.*[8] obtained the cyclotron effective mass $m_c=1.12\,m$ under the same experimental conditions described above. There can be several mechanisms which give rise to the enhancement of the effective mass. The difference of the effective masses of GaAs and $Al_xGa_{1-x}As$ causes a slight mass shift.

Considering $(\hbar^2k^2/2m_z-\hbar^2k^2/2m)$ to the lowest order, we have

$$\frac{\Delta m}{m}\simeq\left(1-\frac{m}{m'}\right)\int_{-\infty}^{0}dz|\zeta_0(z)|^2. \quad (2.5)$$

The shift due to this mechanism increases with N_s because the wave function is pushed toward the $Al_xGa_{1-x}As$ layer for higher electron concentrations. It also depends on the Al content x of the $Al_xGa_{1-x}As$ layer. However, its absolute value turns out to be quite small and contributes to a shift of less than 1% even at $N_s=1.6\times10^{12}$ cm^{-2}. This can be understood from Fig. 1, which shows that the electron density in the $Al_xGa_{1-x}As$ layer is of the order of only 1% of the total. It should be noted, however, that even such a small amplitude of the wave function in the $Al_xGa_{1-x}As$ layer can give rise to a strong scattering due to alloy-disorder in the layer, as will be discussed in a following paper.

The nonparabolicity of the energy dispersion relation present in the conduction band of GaAs is much more important. Since the amplitude of the wave function is extremely small in the $Al_xGa_{1-x}As$ layer, we can obtain a rough estimate of the energy shift as

$$\Delta E_i(k)\simeq\frac{1}{2}E_g\left\{\left[1+\frac{4\langle K\rangle_{ik}}{E_g}\right]^{1/2}-1\right\}, \quad (2.6)$$

where $\langle K\rangle_{ik}$ is the expectation value of the kinetic energy.[12] The effective mass enhancement at the Fermi level becomes

$$\frac{\Delta m}{m}\simeq\left[1+4\frac{\langle K\rangle_0+E_F}{E_g}\right]^{1/2}-1, \quad (2.7)$$

where $\langle K\rangle_i$ is the kinetic energy for the motion perpendicular to the interface and E_F is the Fermi energy measured from the bottom of the lowest subband. Note that the nonparabolicity effect is dominated by the kinetic energy and the potential energy is not important. Note, further, the kinetic energy has only a small amount of contribution to the subband energy. As a matter of fact, the virial theorem shows that $\langle K\rangle_i=E_i/3$ for a triangular potential. The contribution is even smaller for the present self-consistent potential. Combining eqs. (2.5) and (2.7) we have, for example, $\Delta m\sim0.10$ m at the Fermi energy E_F of the lowest subband in the quasi-accumulation case ($N_s=1.6\times10^{12}$ cm^{-2}). This value is slightly smaller than experimentally observed $\Delta m\sim0.12$ m. Calculations for different cases indicate that experimentally observed enhancement[8-11] is always 10~20% larger than the theoretical estimate based on eqs. (2.5) and (2.7). Electron-phonon interactions (polaron effects) might be responsible for such discrepancies. Equation (2.6) can be used also for evaluating subband energy shifts. It turns out that the shift of energy levels is extremely small. This is especially true for subband energy separations for same wave vector k.

§3. Light Scattering Spectra

The two different types of intersubband excitations, the charge-density and the spin-density excitations, are observed in resonant light scattering experiments in $GaAs/Al_xGa_{1-x}As$ heterojunctions.[13-21] In the latter case the spin state of an excited electron is different from the initial state. In the former case, the transition is between same spin states and is accompanied by change in the electron density distribution. Therefore, the charge-density excitation is affected by the depolarization effect and also couples with LO phonons in the GaAs layer. Intersubband excitation spectra have been discussed extensively in space charge layers on Si surfaces.[1,22] To calculate the spectra we neglect differences of phonon spectra in GaAs and $Al_xGa_{1-x}As$ and use those of GaAs only for simplicity. This approximation is justified since the amplitude of the wave function in the $Al_xGa_{1-x}As$ is extremelty small (only 1% for the lowest subband as has been seen and even smaller for excited subbands). Further it is consistent with the neglect of difference in the static dielectric constants of GaAs and $Al_xGa_{1-x}As$. The spectra of the charge-density excitation are determined by[1,7,22]

$$\det|[E_{ji}^2-(\hbar\omega)^2]\delta_{jj'}\delta_{ii'}+A_{(j'i')(ji)}-B_{(jj')(ii')}|=0, \quad (3.1)$$

where $E_{ji}=E_j-E_i$. The matrix A and B are defined as

$$A_{(ji)(j'i')}=2\frac{4\pi e^2}{\varepsilon_L(\omega)}(N_{j'}-N_{i'})^{1/2}(N_{i'}-N_i)^{1/2}E_{j'i'}^{-3/2}E_{ji}^{-3/2}\int dz\left(\frac{\hbar^2}{2m_z}\right)^2(\zeta_j^*\zeta_{i'}'-\zeta_{j'}^{*\prime}\zeta_{i'})(\zeta_j^*\zeta_i'-\zeta_j^{*\prime}\zeta_i), \quad (3.2)$$

and $$B_{(ji)(j'i')}=2(N_{j'}-N_{i'})^{1/2}(N_{i'}-N_i)^{1/2}E_{j'i'}^{-1/2}E_{ji}^{-1/2}\int dz\,\zeta_{j'}^*\zeta_{i'}\zeta_j^*\zeta_i\left(-\frac{\partial v_{xc}}{\partial n}\right), \quad (3.3)$$

where N_j is the electron concentration in the subband j and $\varepsilon_L(\omega)$ is the lattice dielectric function given by

$$\varepsilon_L(\omega)=\kappa_\infty\frac{\omega_l^2-\omega^2}{\omega_t^2-\omega^2}, \quad (3.4)$$

with ω_t and ω_l are the frequency of transverse and longitudinal optical phonons, respectively, and $\kappa=\kappa_\infty\omega_l^2/\omega_t^2$. The matrix A represents the depolarization effect and B the excitonic local field correction taken into account in the local density-functional approximation.[23]

The spectra for the spin-density excitation is determined by

$$\det|[E_{ji}^2-(\hbar\omega)^2]\delta_{j'j}\delta_{i'i}-C_{(j'i')(ji)}|=0. \quad (3.5)$$

Here, the matrix C is defined by

$$C_{(j'i')(ji)}=2(N_{j'}-N_{i'})^{1/2}(N_j-N_i)^{1/2}E_{j'i'}^{-1/2}E_{ji}^{-1/2}\times\int dz\,\zeta_{j'}^*\zeta_{i'}\zeta_j^*\zeta_i\left(-\frac{\partial v_{xc}}{\partial m(z)}\right), \quad (3.6)$$

where $m(z)=n_\uparrow(z)-n_\downarrow(z)$ is the local spin density. The exchange-correlation potential for a spin-polarized electron gas has also been parameterized by Gunnarson and Lundqvist.[5] The excitonic effect on the intersubband excitation is different for the charge-density and spin-density excitations as already noted previously.[24]

Figure 4 gives an example of calculated spectra for the Al content $x=0.3$ and $N_{depl}=5\times10^{10}\,cm^{-2}$. In total 10 subbands are included and eqs. (3.1) and (3.2) are solved numerically. Use has been made of $\hbar\omega_l=36.7$ meV and $\hbar\omega_t=33.6$ meV. The spin-density excitation energy is very close to the corresponding subband energy separation except for the transition from E_0 to E_1. The excitonic effect for the 0→1 transition is about 1 meV around $N_s=5\times10^{11}\,cm^{-2}$ and increases slightly with N_s. The figure demonstrates a strong interaction of intersubband charge-density excitations with the LO phonon when they are close in energy. Above $N_s=7.3\times10^{11}\,cm^{-2}$ additional transitions from the first excited subband appear. Interactions between transitions from the lowest subband and those from the first excited subband are very small.

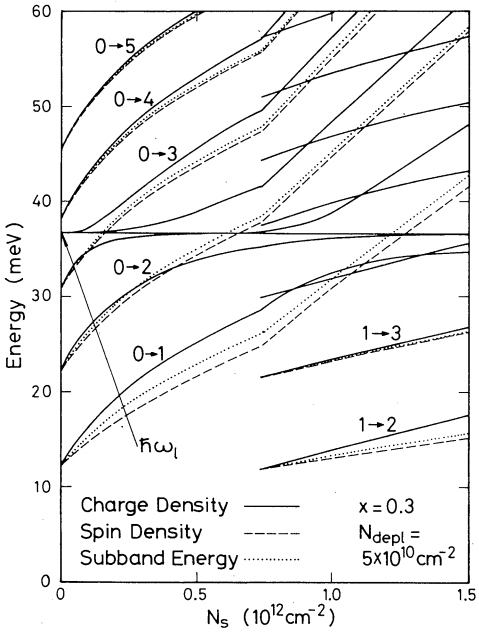

Fig. 4. An example of calculated light-scattering spectra for $N_{depl}=5\times10^{10}\,cm^{-2}$ and $x=0.3$. The solid, and dashed lines represent energies for the charge-density and spin-density excitations, respectively. The dotted lines represent corresponding subband energy separations. The charge-density excitation interacts strongly with LO phonons when their energies are close. Interactions between transitions among different levels are not important.

Figure 5 compares calculated and observed spectra for a quasi-accumulation case ($N_s=6.2\times10^{11}\,cm^{-2}$). The experimental results of Pinczuk and Worlock[20] show two distinct peaks corresponding to the transitions 0→1 and 1→2. Other transitions are broad and not so distinct. In the calculation we have assumed $N_{depl}=5\times10^9\,cm^{-2}$, which is expected to be slightly larger than actual N_{depl} in the quasi-accumulation case. The reason is that very small N_{depl} makes excited subbands higher than the first almost continuum states and the calculation impossible within the present formulation. It is expected that the subband energy separations E_{10} and E_{21} are influenced only a little by such slightly larger N_{depl}. It can be seen that the agreement is satisfactory especially for the 0→1 and 1→2 transitions. Experiments have been reported also by

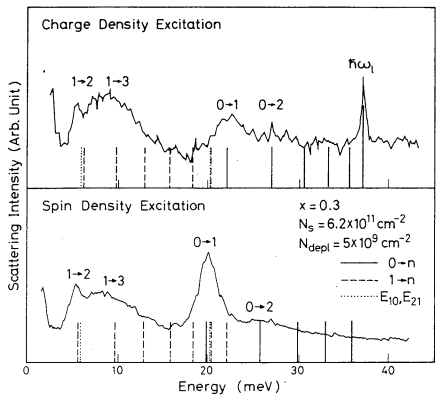

Fig. 5. Comparison of calculated and observed light-scattering spectra in a quasi-accumulation case for $x=0.3$ and $N_s=6.2\times10^{11}$ cm^{-2}. Experiments have been performed by Pinczuk and Worlock.[20] The upper and lower panels represent the charge-density and spin-density excitations, respectively. The vertical solid lines represent calculated resonance energies for transitions from the lowest subband and the dashed lines those for transitions from the first excited subband. The subband energy separations E_{10} and E_{21} are indicated by dotted lines. In the calculation we have assumed $N_{depl}=5\times10^9$ cm^{-2}.

Abstreiter *et al.* for spin-density excitations.[15,16] Their experimental results seem to give much smaller values for the transition energies than the present calculation. The reason of such discrepancies is not known.

§4. Summary and Conclusion

We have calculated the subband structure of a two-dimensional system at GaAs/Al_x-$Ga_{1-x}As$ heterojunction interfaces. Effects of many-body electron-electron interactions are taken into account in the local density-functional approximation and shown to be not so important although not negligibly small. Dynamical nature of electron-phonon interactions has not been included explicitly in calculating subband energies. As for the boundary condition for the envelopes of GaAs and $Al_xGa_{1-x}As$, use has been made of the theory proposed previously, but effects of their discontinuities are shown to be unimportant as expected. The calculated subband structure explains experimental results concerning electron distributions among different subbands. Effects of the nonparabolicity of the GaAs conduction band have also been considered. Its effect on the subband energy turns out to be quite small and can be neglected for practical purposes within the range of experimentally accessible electron concentrations. The enhancement of the effective mass due to the nonparabolicity is slightly smaller than observed in cyclotron resonances.

The spectra of light scatterings caused by intersubband excitations have also been calculated. The charge-density excitation has been shown to be strongly affected by the depolarization effect and interact strongly with LO phonons in GaAs. The excitonic local-field effect reduces the energy of the spin-density excitation slightly from the corresponding subband energy separation. The effect is small but cannot be neglected especially for the transition from the lowest to the first excited subband. The result for a quasi-accumulation case is in reasonable agreement with experimental results.

Acknowledgments

The numerical computation has been performed with the aid of FACOM M200 at the University of Tsukuba. This work is partially supported by the Grant-in-Aid for Scientific Research from the Ministry of Education.

References

1) See, for example, T. Ando, A. B. Fowler and F. Stern: Rev. Mod. Phys. **54** (1982) 437.
2) T. Ando and S. Mori: J. Phys. Soc. Jpn. **47** (1979) 1518.
3) S. Mori and T. Ando: Surf. Sci. **98** (1980) 101.
4) T. Ando and S. Mori: Surf. Sci. **113** (1982) 124.
5) O. Gunnarson and B. I. Lundqvist: Phys. Rev. **B13** (1976) 4274.
6) G. H. Kawamoto, R. Kalia and J. J. Quinn: Surf. Sci. **98** (1980) 589.
7) G. H. Kawamoto, J. J. Quinn and W. L. Bloss: Phys. Rev. **B23** (1981) 1875.
8) H. L. Störmer, R. Dingle, A. C. Gossard, W. Wiegmann and M. D. Sturge: Solid State Commun. **29** (1979) 705; J. Vac. Sci. & Technol. **16** (1979) 1517.
9) H. L. Störmer: *Proc. 15th Int Conf. Phys. Semiconductors, Kyoto, 1980*, J. Phys. Soc. Jpn. **49** (1980) Suppl. A, p. 1013.
10) K. Muro, S. Narita, S. Hiyamizu, K. Nanbu and H. Hashimoto: Surf. Sci. **113** (1982) 321.
11) P. Voisin, Y. Guldner, J. P. Vieren and M. Voos: Appl. Phys. Lett. **39** (1981) 982.
12) Y. Takada and Y. Uemura: J. Phys. Soc. Jpn. **43** (1977) 139.
13) E. Burstein, A. Pinczuk and S. Buchner: *Physics*

of Semiconductors, ed. B. L. H. Wilson (Institute of Physics, Bristol, 1978) p. 1231.
14) E. Burstein, A. Pinczuk and D. L. Mills: Surf. Sci. **98** (1980) 451.
15) G. Abstreiter and K. Ploog: Phys. Rev. Lett. **42** (1979) 1308.
16) G. Abstreiter: Surf. Sci. **98** (1980) 117.
17) A. Pinczuk, H. L. Störmer, R. Dingle, W. Wiegmann and A. C. Gossard: Solid State Sommun. **32** (1979) 1001.
18) A. Pinczuk, J. M. Worlock, H. L. Störmer, R. Dingle, W. Wiegman and A. C. Gossard: Surf. Sci. **98** (1980) 126.
19) A. Pinczuk, J. M. Worlock, H. L. Störmer, R. Dingle, W. Wiegmann and A. C. Gossard: Solid State Commun. **36** (1980) 43.
20) A. Pinczuk, J. M. Worlock, H. L. Störmer, A. C. Gossard and W. Wiegmann: J. Vac. Sci. & Technol. **19** (1981) 561.
21) A. Pinczuk and J. M. Worlock: Surf. Sci. **113** (1982) 69.
22) D. A. Dahl and L. J. Sham: Phys. Rev. B**16** (1977) 651.
23) T. Ando: Z. Phys. B**26** (1977) 263.
24) T. Ando, E. Eda and M. Nakayama: Solid State Commun. **23** (1977) 751.